



## Synthesis and Characterization of New Thiazine Compounds Derivatized From 1-(Pyrazin-2-Yl)-3-(Benzylidene) Propanone and Study of Their Biological Effectiveness

Saad Salim Jasim<sup>1</sup>, Shakhawan Beebany<sup>2\*</sup>, Jawdat Hilmi Abdulwahid<sup>3</sup>,  
Khalid A. Al-Badrani<sup>4</sup>

<sup>1,2</sup> Department of Chemistry- College of Sciences- University of Kirkuk,  
Kirkuk, 36001, Iraq.

<sup>3</sup> Environmental and Pollution Engineering Department, Technical Engineering College,  
Northern Technical University of Kirkuk, Kirkuk, 36001, Iraq.

<sup>4</sup> Department of Chemistry- College of Education for Pure Sciences,  
University of Tikrit, Tikrit, 34001, Iraq.

Email : <sup>1</sup>[saadsalem@uokirkuk.edu.iq](mailto:saadsalem@uokirkuk.edu.iq) <sup>2\*</sup>[sh.beebany@uokirkuk.edu.iq](mailto:sh.beebany@uokirkuk.edu.iq)  
<sup>3</sup>[jawdat.1965@ntu.edu.iq](mailto:jawdat.1965@ntu.edu.iq) <sup>4</sup>[khalidalbadrany477@tu.edu.iq](mailto:khalidalbadrany477@tu.edu.iq)

**Abstract.** This study examines the synthesis and characterization of new compounds produced from chalcone, confirming their favorable yield and excellent purity utilizing Using FT-IR and <sup>1</sup>H and <sup>13</sup>C NMR spectroscopy. The compounds showed efficacy comparable to that of conventional antibiotics, demonstrating substantial bactericidal activity against *Staphylococcus aureus* and *Escherichia coli*. Interestingly, molecule S10 had stronger antibacterial activity, possibly as a result of its efficient electronic pairings. Furthermore, the compounds demonstrated resilience for up to 45 seconds when tested for stability under helium-neon laser irradiation. Longer exposure (60 seconds), however, caused discernible color and melting point alterations, suggesting thermal or photochemical deterioration. These results point to the possibility of additional pharmacological uses for molecules produced from chalcone.

**Keywords:** Heterocyclic Compounds, Chalcone Derivatives, Antibacterial Efficacy, Thiazine, Biological Activity.

### 1. INTRODUCTION

Chalcones are composed of an electrophilic  $\alpha,\beta$ -unsaturated carbonyl structure in which the carbonyl atom is in a prolonged conjugation with a neighboring olefinic bond [1]. In order to create a molecular structure of deep resonance stability, this complex electronic delocalization coordinates the structural attachment of an aromatic entity at the  $\alpha$ -position (next to the enone system) and another aryl moiety at the  $\beta$ -position. Chalcone derivatives play a crucial role in a wide range of scientific fields because of this  $\pi$ -conjugated system, particularly in the field of complex chemical synthesis [2], the vast pharmaceutical industry [3], and the regulation of many bioactivities [4]. Heterocyclic compounds, which are defined by cyclic structures that include heteroatoms like oxygen, sulfur, or nitrogen, are ubiquitous in nature and are essential building blocks for industrial and medical chemistry. These structurally adaptable substances serve as essential building blocks for the biosynthesis of polypeptides, enzymes, saccharides and their derivatives, and nucleotidic macromolecules [5]. These compounds can be categorized according to the type and quantity of heteroatoms contained in the cyclic nucleus because of their inherent heteroatomic makeup [6]. The nucleophilic condensation of chalcone precursors with thiourea yields thiazine, a six-membered heterocycle

consisting of a sulfur atom, a nitrogen heteroatom, and a tetravalent carbonaceous backbone [7].

Due to their proven antibacterial efficacy [8], cytotoxic potential against neoplastic diseases [9], and strong anti-inflammatory qualities [10], these heterocyclic frameworks have attracted a lot of pharmacological attention, especially in the context of therapeutic interventions.

The goal of the current study is to carefully synthesize heterocyclic systems from chalcone scaffolds and then assess their biological activity against bacterial strains that are resistant to Gram staining methods.

## 2. MATERIALS AND METHODS

### Preparation of Chalcones Derivatives (S1-S5) [11]

In an ethanolic solution (10 mL), a carefully measured amount of acetylpyrazine (0.005 mL, 0.61 g) was systematically combined with equimolar concentrations of several p-substituted benzaldehyde derivatives (0.005 mL) while being vigorously stirred. To ensure uniform dispersion and long-lasting nucleophilic activation, aqueous sodium hydroxide (10% w/v) was added to the reaction milieu dropwise. In order to promote aldol condensation, the reaction mixture was continuously stirred for 6–7 hours at carefully regulated temperatures (20–40°C). To cause the precipitation of the resulting chalcone analogs, the reaction system was concentrated using controlled solvent evaporation after it was finished. To improve purity and structural integrity, the resulting solid-phase product was carefully separated using vacuum filtration, then dried and recrystallized from ethanol in stages. Thin-layer chromatography (TLC) was used to carefully track the reaction kinetics and product production. Table 1. provides a detailed description of the physicochemical characteristics of the produced compounds (S1–S5).

**Table (1):** Physical properties of compounds (S1-S5).

Com. No.	X	Molecular formula	M.P °C	Yield%	Color
S <sub>1</sub>	H	C <sub>13</sub> H <sub>9</sub> N <sub>2</sub> O	160-165	87	Off White
S <sub>2</sub>	Br	C <sub>13</sub> H <sub>9</sub> N <sub>2</sub> OBr	135-140	90	Light Brown
S <sub>3</sub>	Cl	C <sub>13</sub> H <sub>9</sub> N <sub>2</sub> OCl	150-160	85	Dark Brown
S <sub>4</sub>	F	C <sub>13</sub> H <sub>9</sub> N <sub>2</sub> OF	145-150	75	Yellow
S <sub>5</sub>	NO <sub>2</sub>	C <sub>13</sub> H <sub>9</sub> N <sub>3</sub> O <sub>3</sub>	130-140	87	Off White

### Preparation of Thiazine Derivatives (S6-S10) [12]

In a 10 mL ethanolic environment, equimolar proportions (0.001 mol) of the synthesized chalcone and thiourea were subjected to nucleophilic condensation. A catalytic

volume (10 mL) of 10% sodium ethoxide served as a potent Brønsted base to aid in deprotonation and the subsequent formation of enolate. To achieve the highest level of enamionone intermediate stability, the reaction matrix was exposed to continuous heat reflux for six hours. To encourage controlled crystallization, the resulting mixture was cooled to room temperature gradually after the reaction and then quenched in pulverized ice. Then, to improve product formation by thermodynamically preferred lattice structuring, the system was chilled for 48 hours. After that, a 10% hydrochloric acid solution was carefully used for neutralization in order to adjust the pH and precipitate the desired heterocyclic entity. As shown in Table (2), the resultant crude precipitate underwent vacuum filtering, successive desiccation, and careful recrystallization.

**Table (2):** Physical properties of compounds (S<sub>6</sub>-S<sub>10</sub>).

Com. No.	X	Molecular formula	M.P °C	Yield%	Color
S <sub>6</sub>	H	C <sub>14</sub> H <sub>12</sub> N <sub>4</sub> S	187-189	67	Yellow
S <sub>7</sub>	Br	C <sub>14</sub> H <sub>11</sub> BrN <sub>4</sub> S	231-233	71	Orange
S <sub>8</sub>	Cl	C <sub>14</sub> H <sub>11</sub> ClN <sub>4</sub> S	212-214	73	White
S <sub>9</sub>	F	C <sub>14</sub> H <sub>11</sub> FN <sub>4</sub> S	216-218	64	Orange
S <sub>10</sub>	NO <sub>2</sub>	C <sub>14</sub> H <sub>11</sub> N <sub>5</sub> O <sub>2</sub> S	191-102	75	Brown

### Biological Activity Study

Both Gram-positive and Gram-negative staining properties are displayed by *S. aureus*, but *E. coli* is the bacterial strain used in this investigation. For bacterial growth, molten Hinton Agar has been used as a selective and differential culture medium. Dimethyl sulfoxide (DMSO) was used as an organic solvent to create chemical solutions with the specified chalcone derivatives (S<sub>6</sub>–S<sub>10</sub>), resulting in serial dilutions at concentrations of 0.01–0.001 and 0.0001 mg/mL [13,14].

A thorough quantitative evaluation was used to determine the minimal inhibitory concentration (MIC). The standard nutrient-rich matrix used was Mueller-Hinton agar, and the antibiotic susceptibility of the bacterial isolates under study was assessed using an agar well-diffusion experiment. After the media was prepared, it was carefully sterilized before being aliquoted into sterile Petri plates, where it was left to harden under carefully monitored aseptic conditions. Each plate was then aseptically pierced with four equally spaced wells [15].

To promote bacterial growth and compound diffusion, the infected plates were incubated for 24 hours at the ideal temperature of 37°C. The diameter of the zones of inhibition surrounding each well was used to estimate the synthetic compounds' antibacterial efficacy. The diffusion radius, a measure of the derivative's bioactivity, was directly correlated with the degree of bacterial growth suppression. Similar to the inhibitory mechanisms found in

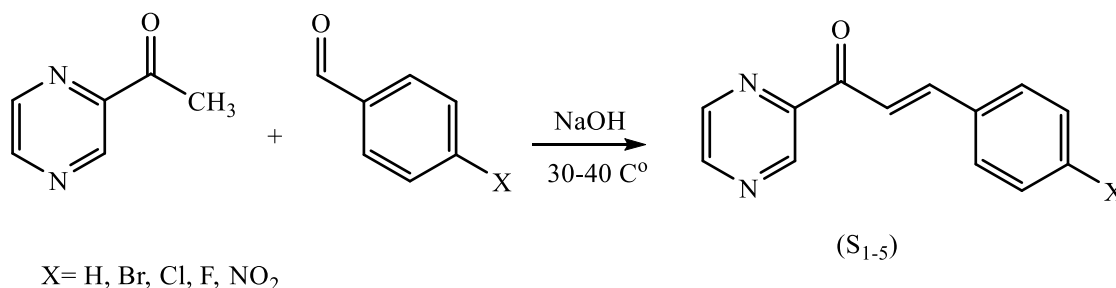
traditional antibiotic drugs, a larger zone of inhibition indicated improved antimicrobial activity [16,17].

### 3. RESULTS AND DISCUSSIONS

#### Synthesis and Characterization of Chalcones (S1-S5)

##### Analysis Data

Chalcones (S1-S5) were prepared by reacting acetylpyrazine with p-substituted benzaldehyde in a basic medium as in the equation below:



After carefully examining the infrared (IR) absorption profiles of substances (S1–S5) using spectroscopy, a unique vibrational band was identified in the 3074–3039 cm<sup>-1</sup> spectral window. This band was attributed to the stretching oscillations of aromatic C–H moieties. The absorption maxima of the ketonic carbonyl (C=O) functional group also showed a noticeable hypsochromic shift, appearing in the spectral range of 1689–1662 cm<sup>-1</sup>. The large conjugative delocalization resulting from the electronic interaction between the carbonyl and the nearby α,β-unsaturated olefinic system, which itself displayed a diagnostic vibrational signal between 1613 and 1587 cm<sup>-1</sup>, is responsible for this wavenumber reduction.

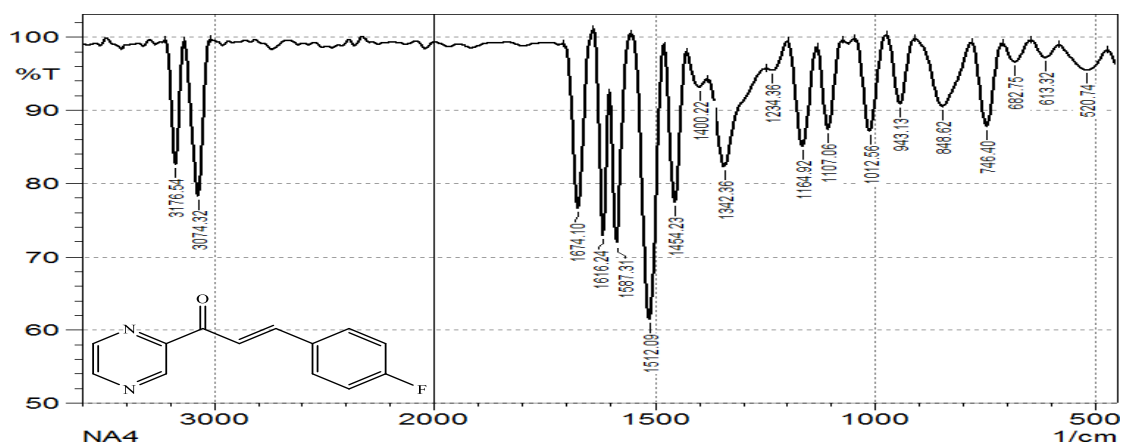
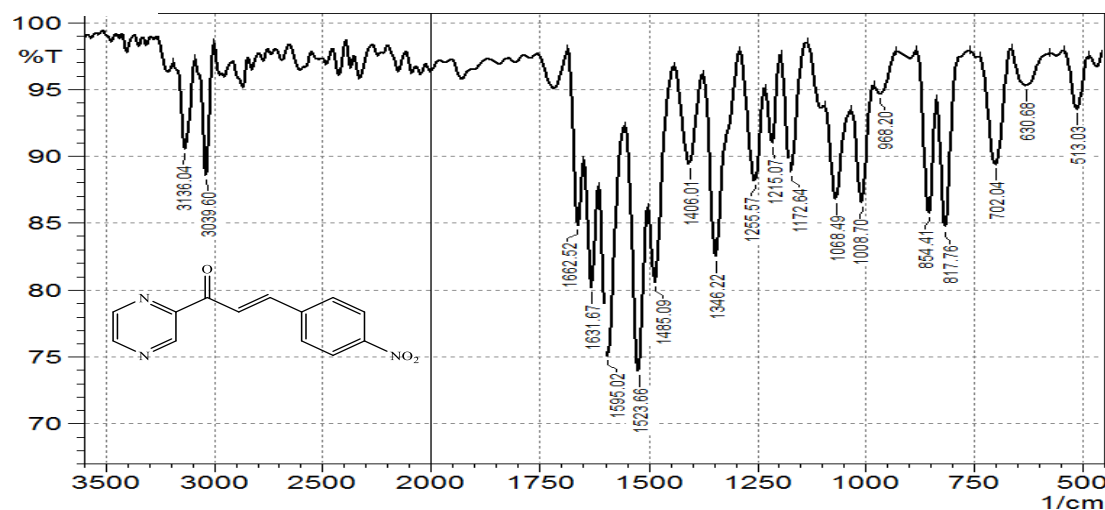
Furthermore, the stretching vibrational mode of the alkenic (=C–H) moiety was clearly identified as the source of an absorption band seen in the spectral region of 3176–3135 cm<sup>-1</sup>. Additionally, the spectroscopic profile showed the presence of a distinctive absorption band between 1647 and 1616 cm<sup>-1</sup>, which corresponds to the imine (C=N) functional group's stretching vibrations. Furthermore, two strong absorption bands were identified in the IR spectrum at 1558–1512 cm<sup>-1</sup> and 1490–1454 cm<sup>-1</sup>. These bands were attributed to the vibrational stretching modes of conjugated aromatic (C=C) frameworks.

These empirical observations show significant congruence with spectroscopic data presented in the existing literature [18], as supported by Table (3) and Figures (1 & 2).

**Table (3):** Results of infrared absorption of Chalcones (S<sub>1</sub>-S<sub>5</sub>).

Com. No.	X	IR (KBr) cm <sup>-1</sup>						
		□(C-H) Ar	□(=C-H)	□ C=O	□(C=C)	□(C=C) Ar	ν C=N	Other absorptions
S <sub>1</sub>	H	3066	3135	1676	1610	1558-1470	1639	□(C-H) 2929-2972

S <sub>2</sub>	Br	3055	3165	1687	1611	1556-1483	1632	□(C-Br) 675
S <sub>3</sub>	Cl	3045	3150	1689	1613	1548-1490	1647	□(C-C) 744
S <sub>4</sub>	F	3074	3176	1674	1587	1512-1454	1616	□(C-F) 943
S <sub>5</sub>	NO	3039	3136	1662	1595	1523-1485	1631	□(N-O) as
	2							a sy.1576. sy1346

Figure (1): FT-IR Spectra of compound (S<sub>4</sub>).Figure (2): FT-IR Spectra of compound (S<sub>5</sub>).

The vinylic proton (O=C-CH) in intimate electronic conjugation with the carbonyl moiety is clearly responsible for the unique resonance that appears in the  $\delta$  6.66–6.69 ppm area of the molecule (S<sub>2</sub>)'s <sup>1</sup>H NMR spectrum data when it is carefully examined in deuterated dimethyl sulfoxide (DMSO-d<sub>6</sub>). Furthermore, the identification of an additional signal at  $\delta$  6.90 and 6.93 ppm indicates the presence of the olefinic proton (=CH) next to the aromatic benzene structure. As seen in Figure 3, the remaining HDO signal (partially deuterated water) is responsible for a singlet resonance at  $\delta$  3.34 ppm, but the solvent's intrinsic methyl protons (DMSO-d<sub>6</sub>) are associated with a clear peak at  $\delta$  2.49 ppm.

A strong downfield resonance at  $\delta$  185.64 ppm in the molecule (S<sub>2</sub>)'s <sup>13</sup>C NMR spectra, which was obtained in DMSO-d<sub>6</sub>, is clearly indicative of the carbonyl carbon (C=O),

confirming its electrophilic character. The olefinic carbon (=CH) next to the enone system is identified by a clear signal at  $\delta$  115.32 ppm, whereas the  $sp^2$ -hybridized carbon (=CH) immediately conjugated to the benzene ring is identified by the appearance of a resonance at  $\delta$  148.30 ppm. Additionally, the methyl-substituted carbons of the pyrimidine moieties are responsible for the signals at  $\delta$  159.57 ppm and  $\delta$  155.38 ppm, indicating their existence within the heterocyclic core. Multiple resonances, which are indicative of aromatic ring carbons in conjugation with the heterocyclic system, are present in the spectral window that spans  $\delta$  122.30–159.57 ppm. Furthermore, the solvent-derived carbon (DMSO- $d_6$ ) is identified by a signal that falls between  $\delta$  39.11 and 40.78 ppm. The detailed spectral explanation is shown in Figure 4.

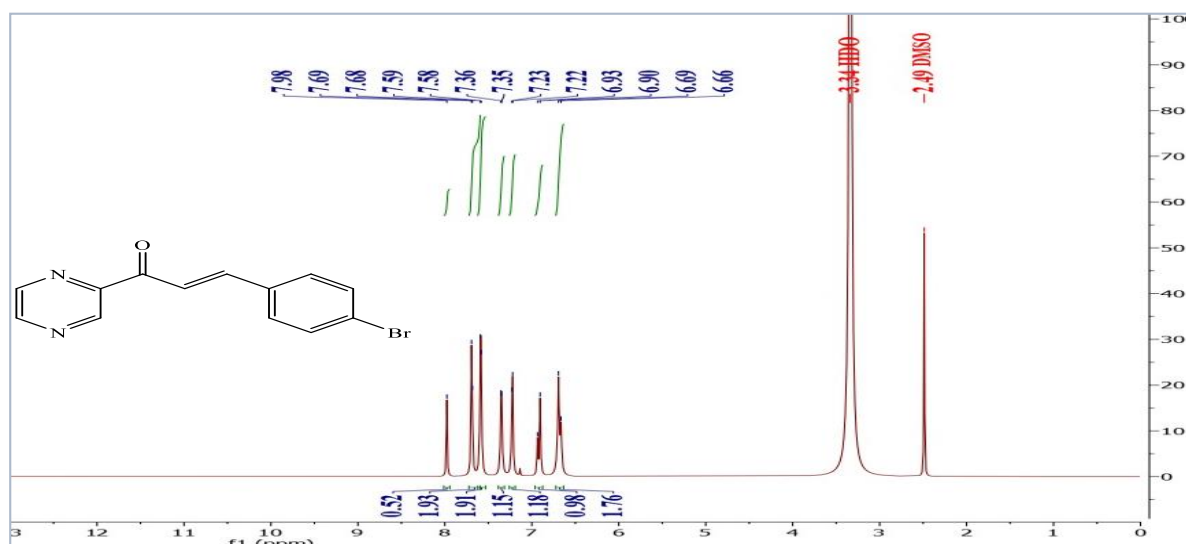


Figure (3):  $^1\text{H-NMR}$  spectrum of the compound ( $S_2$ ).

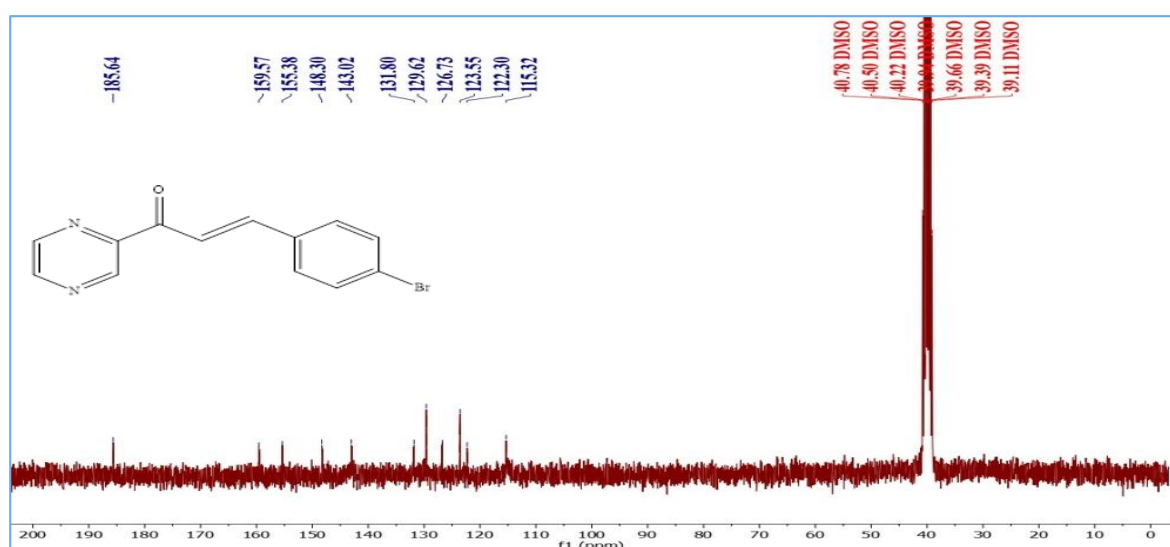
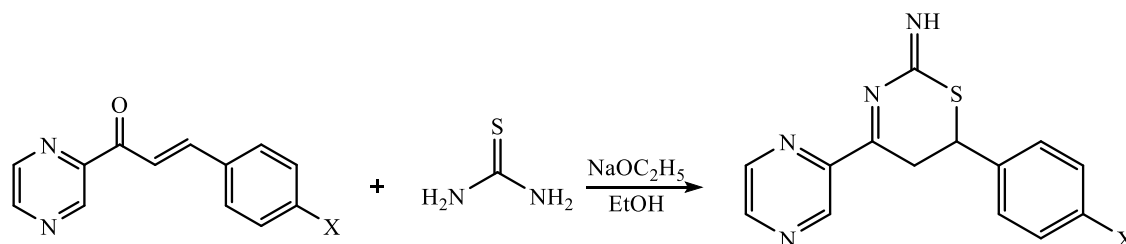


Figure (4):  $^{13}\text{C-NMR}$  spectrum of the compound ( $S_2$ ).

## Synthesis and Characterization of Thiazine Compounds (S6-S10)

The thiazine derivatives (S6-S10) have been prepared as shown in the following equation:



X= H, Br, Cl, F, NO<sub>2</sub>

The structural integrity of the thiazine heterocycle was demonstrated by distinctive vibrational transitions that were clarified by the FT-IR spectroscopic investigation. The presence of the imine linkage within the thiazine core was confirmed by the unambiguous attribution of a prominent absorption band within the spectral domain of 1621–1639 cm<sup>-1</sup> to the stretching vibration of the azomethine (C=N) functional moiety. Furthermore, the aromatic C–H stretching mode was identified as the source of an absorption band that reflected the electrical environment of the aryl substituents and appeared in the 3016–3073 cm<sup>-1</sup> area. Additionally, the spectral fingerprint showed a large absorption resonance in the 3268–3228 cm<sup>-1</sup> band that corresponded to the N–H stretching vibration and was suggestive of tautomeric equilibrium or hydrogen-bonding interactions.

Additionally, the spectral deconvolution identified two separate absorption bands that span the areas 2952–2918 cm<sup>-1</sup> and 2900–2843 cm<sup>-1</sup>, respectively, and are ascribed to aliphatic C–H stretching vibrations. The aromatic system's  $\pi$ -electron delocalization was seen in two absorption bands in the 1560–1512 cm<sup>-1</sup> and 1467–1486 cm<sup>-1</sup> areas, which were attributed to C=C stretching vibrations. Significantly, the C–S stretching vibration was identified as a distinctive absorption feature in the 773–751 cm<sup>-1</sup> range, supporting the structural integration of the thiazine sulfur molecule 19 19. These chemical assignments are supported by the spectrum data, which are methodically gathered in Table (4) and shown in Figures (5) and (6).

**Table (4):** Results of infrared absorption of Thiazine derivatives (S<sub>6</sub>-S<sub>10</sub>).

Com. No.	X	IR (KBr) cm <sup>-1</sup>						
		□(C-H) Ar	□(C-H) Aliph.	□(N-H)	□(C-S)	□(C=C) Ar	ν C=N	Other absorptions
S <sub>6</sub>	H	3016	2918 2875	3228	756	1562,1477	1639 1618	--
S <sub>7</sub>	Br	3063	2931 2872	3265	773	1512,1467	1637 1604	□(C-Br) 557

S <sub>8</sub>	Cl	3024	2950 2843	3261	764	1531,1481	1636 1614	□(C-Cl) 716
S <sub>9</sub>	F	3073	2952 2900	3252	759	1558,1479	1633 1610	□(C-F) 919
S <sub>10</sub>	NO <sub>2</sub>	3061	2945 2865	3268	751	1560,1486	1621 1603	□(N-O) as a sy.1521. sy1323

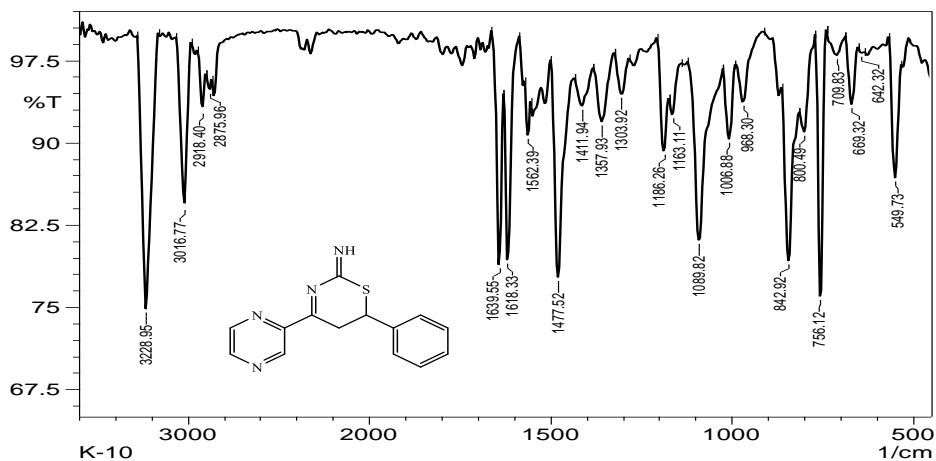


Figure (5): FT-IR Spectra of

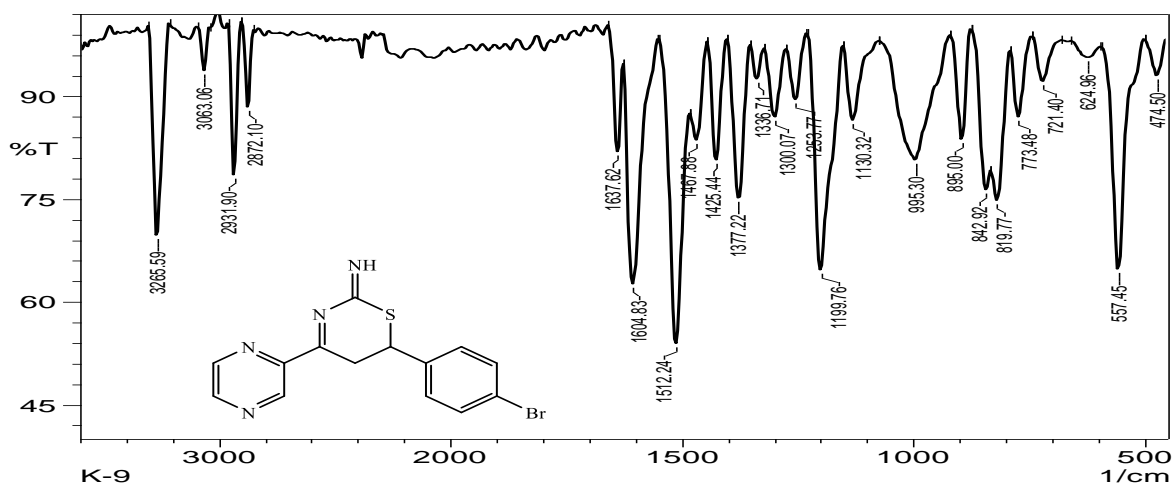
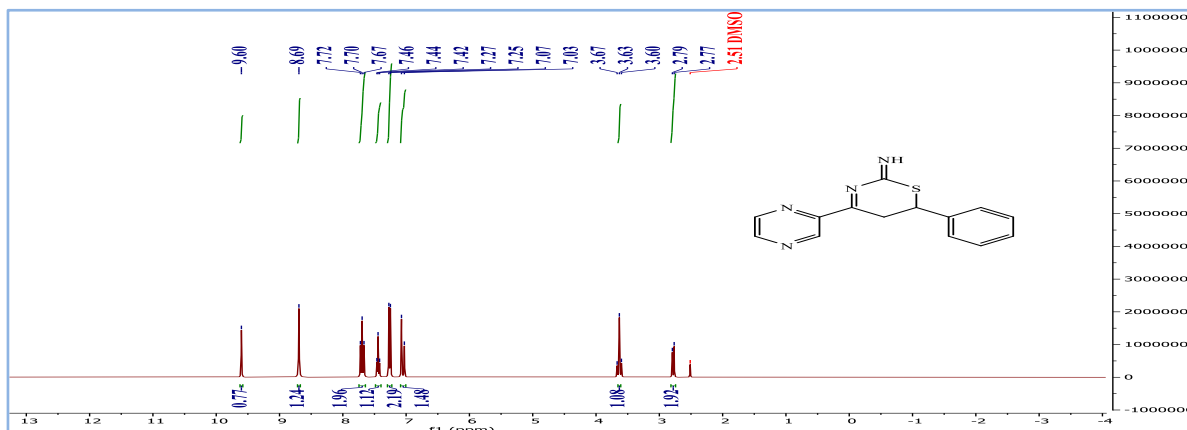


Figure (6): FT-IR Spectra of compound (S<sub>7</sub>).

<sup>1</sup>H NMR spectral analysis of Compound (S<sub>6</sub>) reveals a deshielded resonance at 9.60 ppm that is unmistakably attributed to the NH proton and suggests either intramolecular hydrogen bonding or electronic delocalization effects. The aromatic proton environment is represented by a variety of resonances in the 7.03–8.69 ppm range, which are impacted by changes in  $\pi$ -electron density.

The C-H proton in the thiazine moiety exhibits a distinct triplet signal in the 3.60–3.69 ppm band, which supports the heteroatomic framework's ability to deshield it spatially. The CH<sub>2</sub> protons of the thiazine ring are responsible for the appearance of a doublet resonance at

2.77 and 2.79 ppm, which is suggestive of diastereotopic splitting brought on by limited conformational mobility. Furthermore, as an internal reference, a singlet at 2.51 ppm coincides with the DMSO- $d_6$  solvent's residual proton resonance. For spectral visualization, see Figure (7).



**Figure (7):  $^1\text{H}$  NMR spectrum of the compound ( $S_6$ )**

The amide-like (NH) proton is clearly responsible for the deshielded resonance at 8.99 ppm in the  $^1\text{H}$  NMR spectrum elucidation of substance ( $S_9$ ), indicating that it is involved in hydrogen bonding or electronic deshielding processes. Aromatic proton environments are characterized by a complex multiplicity of resonances that cover the 7.22–8.63 ppm domain. These resonances are probably caused by the  $\pi$ -electron-rich framework. The methine (CH) proton in the thiazine heterocycle is identified by the presence of a triplet signal in the 3.97–4.02 ppm range, whereas the methylene ( $\text{CH}_2$ ) protons of the same ring system are identified by a detectable doublet at 3.00 and 3.02 ppm, which is indicative of its limited electronic environment. Furthermore, the leftover proton signal of the DMSO- $d_6$  solvent, which acts as an internal reference, is responsible for the downfield resonance detected at 2.51 ppm. Figure (8) provides an illustration of these spectral allocations.

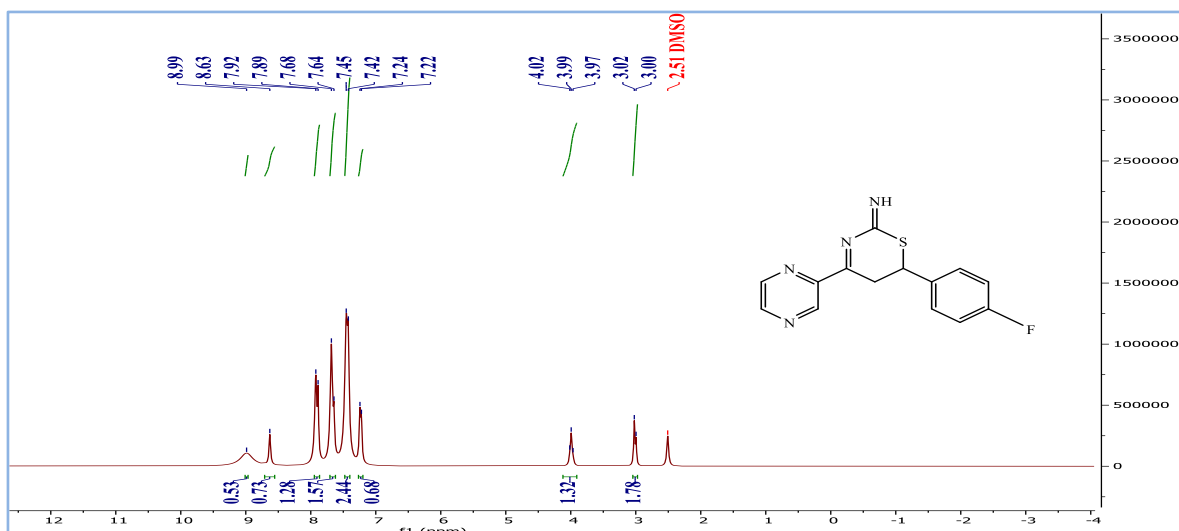


Figure (8): <sup>1</sup>H NMR spectrum of the compound (S<sub>6</sub>)

The carbon resonance associated with the methylene group (CH<sub>2</sub>) in the resulting heterocyclic ring was clearly visible as a signal at  $\delta$  29.06 ppm upon the examination of the chemical (S<sub>6</sub>) <sup>13</sup>C NMR spectra. Furthermore, the methine carbon (CH) of the same cyclic structure was usually identified as the source of a resonance at  $\delta$  65.04 ppm. The signals in the  $\delta$  128.07 to  $\delta$  142.71 ppm chemical shift range are often attributed to the carbons in the aromatic ring system, but the signal at  $\delta$  163.71 ppm was attributed to the carbonylimine (C=N) moiety of the heterocyclic ring. Additionally, the resonance at  $\delta$  168.75 ppm implicated the imidic carbon (C=NH). Dimethyl sulfoxide (DMSO), the solvent, was also visible, with distinctive signals showing up in the  $\delta$  39.23–40.48 ppm region. The portrayal in Figure 9 is consistent with these spectral data.

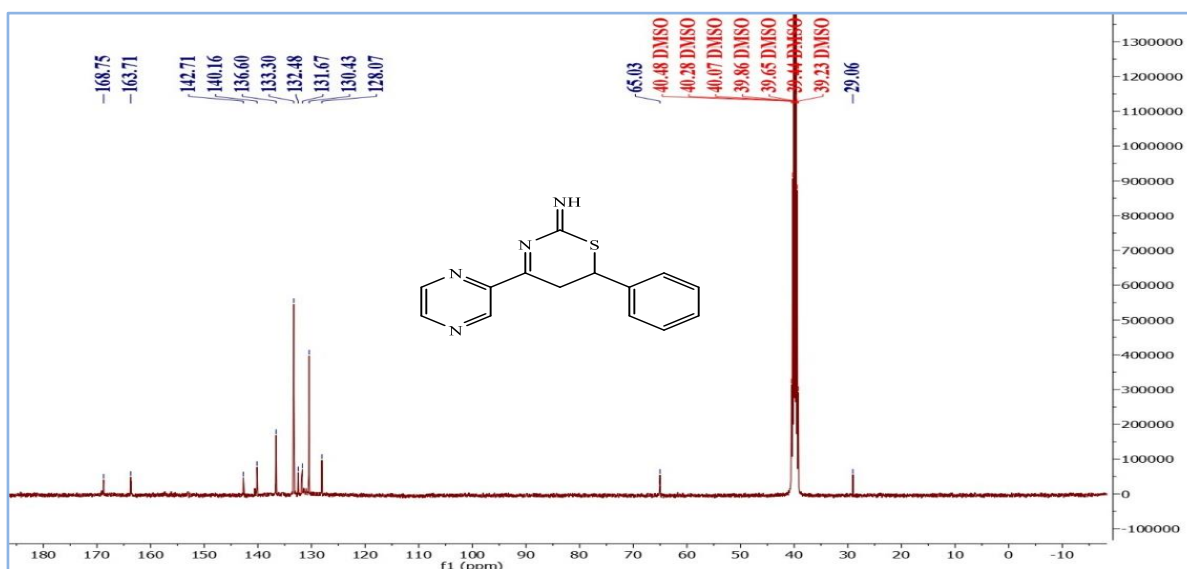


Figure (9): <sup>13</sup>C NMR spectrum of the compound (S<sub>6</sub>)

A careful examination of the compound's (S9)  $^{13}\text{C}$  NMR spectra reveals a clear resonance at 26.68 ppm that corresponds to the methylene carbon ( $\text{CH}_2$ ) of the resulting heterocyclic ring. Methine carbon ( $\text{CH}$ ) in the same ring structure is generally responsible for a signal at 60.49 ppm. In accordance with their usual chemical surroundings, the aromatic carbons in the conjugated ring system display resonances in the spectral window of 128.68 to 141.35 ppm. The resulting heterocycle's carbonyl carbon ( $\text{C}=\text{N}$ ), which is a marker of imine functionality, is strongly signaled at 167.44 ppm, whilst the carbon ( $\text{C}=\text{NH}$ ), which is connected to the azomethine group, is responsible for the resonance at 171.05 ppm. Furthermore, as is typical of its solvent peaks, the solvent DMSO resonates at the 39.30 to 40.56 ppm area. Figure 10 provides a visual representation of the spectrum data.

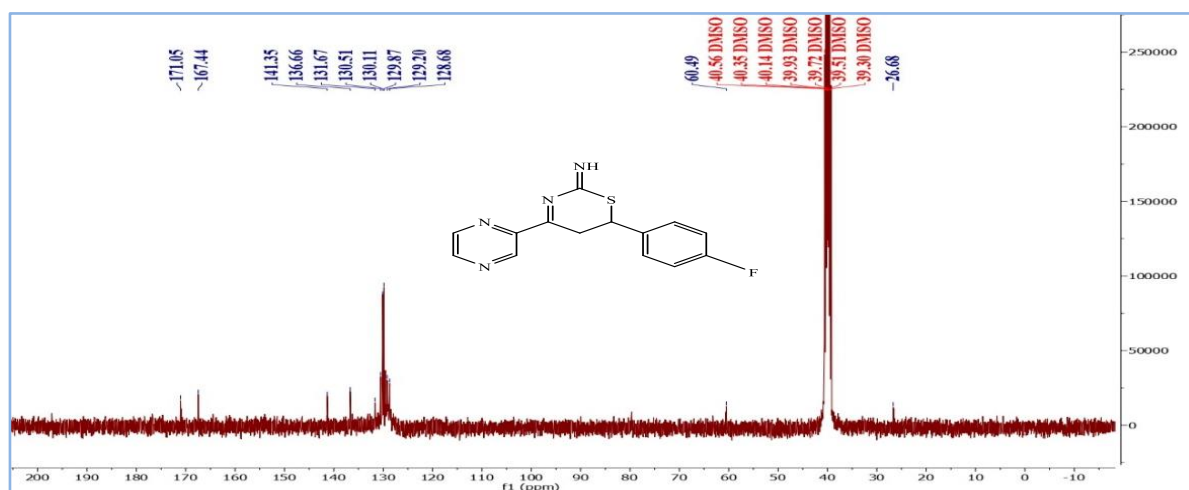
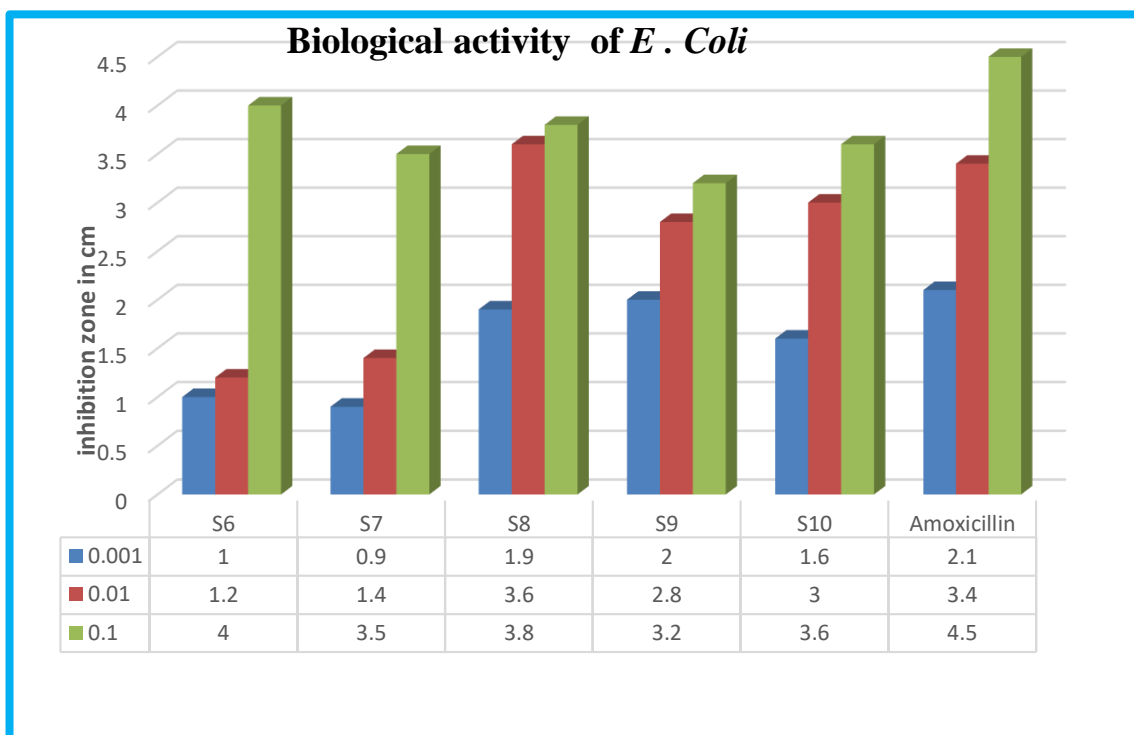


Figure (9):  $^{13}\text{C}$  NMR spectrum of the compound (S.)

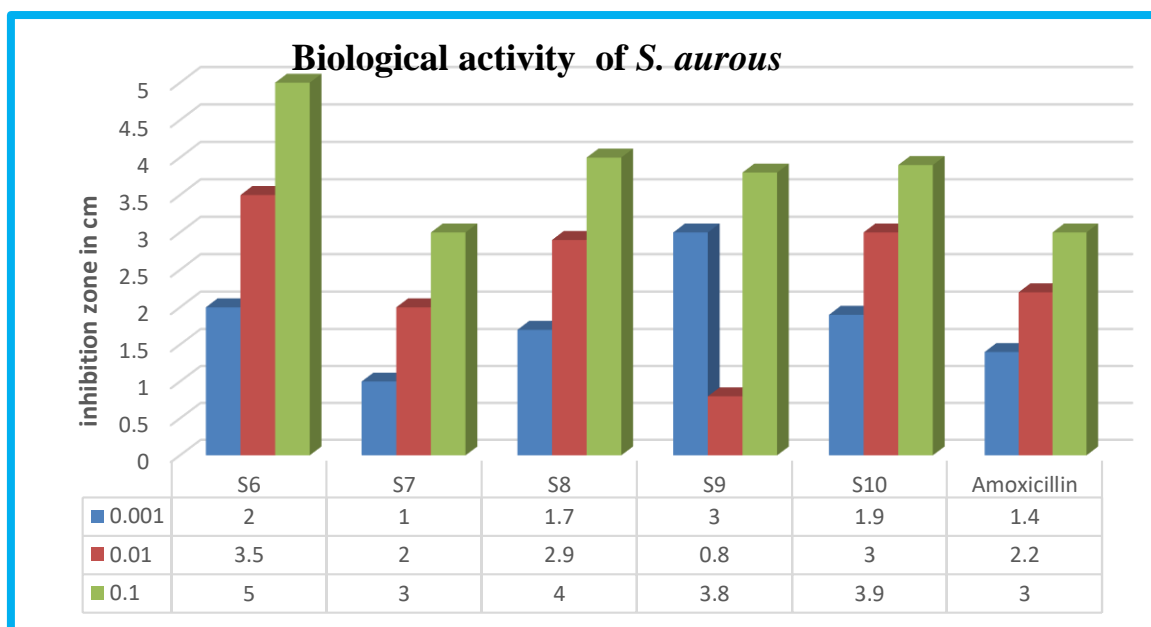
### Evaluation of Biological Activity

Antimicrobial screening was performed on the synthetically generated chemicals used in this study against two different bacterial strains: the Gram-positive *S. epidermidis* and the Gram-negative *E. coli*. The agar diffusion method, as described in the literature [20,21], was used to perform the antimicrobial experiments. The Mueller-Hinton agar was used as the food medium for the bacterial cultures, and the zones of inhibition, measured in centimeters, were carefully recorded for a selection of the produced compounds at concentrations of 0.1, 0.01, and 0.001 mg/mL. These substances' inhibitory effects were compared to those of common antibiotics. Interestingly, the outcomes were compared to the effectiveness of well-known pharmaceutical medicines [22, 23]. While some compounds showed strong selective activity against one bacterial species compared to another, highlighting their possible specificity for either Gram-positive or Gram-negative bacteria, others showed differential bacteriostatic or bactericidal effects on *E. coli* versus *S. epidermidis*. The investigation's findings demonstrated

unique antibacterial qualities, as demonstrated by the differing levels of inhibition seen in several bacterial species [24,25]. The results obtained are further clarified by comprehensive schematics (Schemes 1 & 2) and graphical representations (Figures 10 & 11).



**Scheme (1):** Inhibitory activity of (S<sub>6-10</sub>) for *E. Coli*.



**Scheme (2):** Inhibitory activity of (S6-10) for *S. Aureus*.

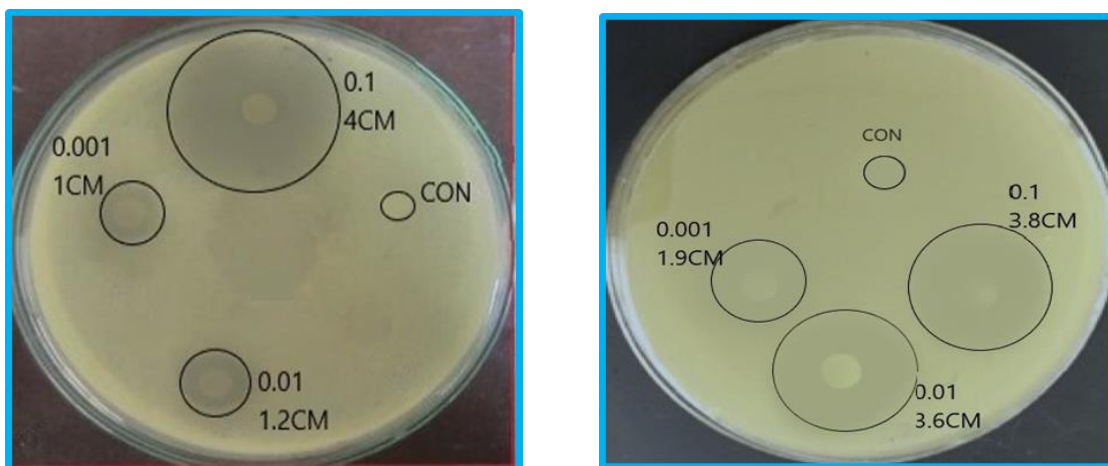


**Figure 10:** Biological effectiveness of the compounds (S<sub>6</sub>, S<sub>9</sub>) against bacterial *S. aureus*.

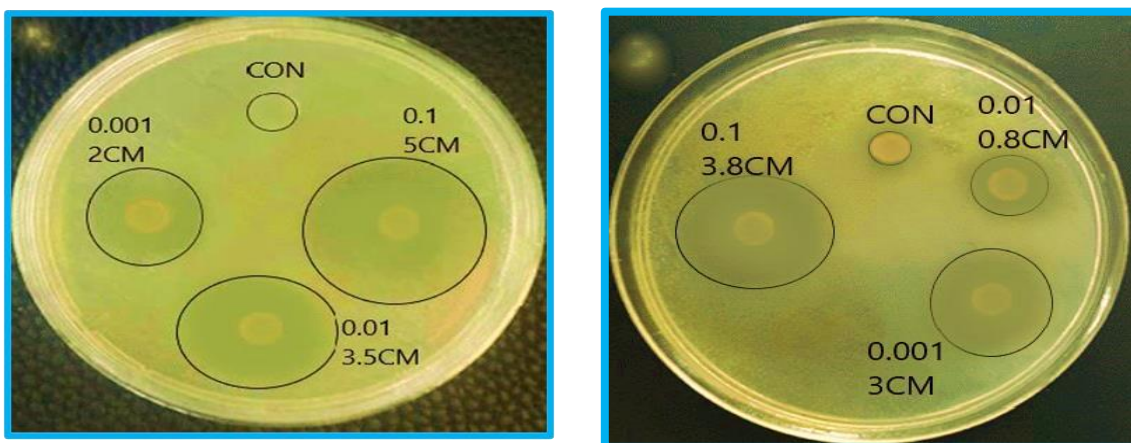


**Figure 11:** Biological effectiveness of the compounds (S<sub>6</sub>, S<sub>9</sub>) against *E. Coli* bacterial.

#### 4. CONCLUSIONS

The formulations' high purity and advantageous yield were confirmed by FT-IR and <sup>1</sup>H and <sup>13</sup>C NMR spectroscopy. They had strong bactericidal action that was almost on par with antibiotics. Because of its efficient electrical pairings, compound S10 showed the maximum efficacy. For up to 45 seconds, the compounds remained stable when exposed to helium-neon lasers. However, after 60 seconds of exposure, color and melting point changes happened, most likely as a result of the extended laser irradiation producing thermal or photochemical changes.

#### REFERENCES

- [1] D.N. Dhar, "The Chemistry of Chalcones and Related Compounds", John Wiley and Sons, Inc., p. 54-47, (1981). ISBN 0471080071.
- [2] Al-Tufah, M.M., Beebaeny, S., Jasim, S.S. and Mohammed, B.L., 2023. Synthesis, characterization of ethyl dioxoisindoliny cyclohexenone carboxylate derivatives from some chalcones and its biological activity assessment. *Chemical Methodologies*, 7, pp.408-418. <https://doi.org/10.22034/chemm.2023.388126.1654>

- [3] Gutierrez, R.M.P., Muñiz-Ramirez, A. and Saucedo, J.V., 2015. The potential of chalcones as a source of drugs. *African Journal of Pharmacy and Pharmacology*, 9(8), pp.237-257. <https://doi.org/10.5897/AJPP2015.%204267>
- [4] Hu, D., Zhang, N., Zhang, Y., Yuan, C., Gong, C., Zhou, Y. and Xue, W., 2023. Design, synthesis and biological activity of novel chalcone derivatives containing indole. *Arabian Journal of Chemistry*, 16(6), p.104776. <https://doi.org/10.1016/j.arabjc.2023.104776>
- [5] Al-Mulla, A., 2017. A review: biological importance of heterocyclic compounds. *Der Pharma Chem*, 9(13), pp.141-147. Available online at [www.derpharmachemica.com](http://www.derpharmachemica.com)
- [6] Amin, A., Qadir, T., Sharma, P.K., Jeelani, I. and Abe, H., 2022. A review on the medicinal and industrial applications of N-containing heterocycles. *The Open Medicinal Chemistry Journal*, 16(1). <http://dx.doi.org/10.2174/18741045-v16-e2209010>
- [7] Asif, M., Imran, M. and Abida, 2022. Antimicrobial activities of various thiazine based heterocyclic compounds: a mini-review. *Mini-Reviews in Organic Chemistry*, 19(2), pp.166-172. <https://doi.org/10.2174/1570193X18666210629102447>
- [8] Choudhary, S., Silakari, O. and Singh, P.K., 2018. Key updates on the chemistry and biological roles of thiazine scaffold: a review. *Mini Reviews in Medicinal Chemistry*, 18(17), pp.1452-1478. <https://doi.org/10.2174/1389557518666180416150552>
- [9] Chaucer, P. and Sharma, P.K., 2020. Study of thiazines as potential anticancer agents. *Plant Arch*, 20(2), pp.3199-3202.
- [10] Wiatrak, B., Krzyżak, E., Szcześniak-Sięga, B., Szandruk-Bender, M., Szelağ, A. and Nowak, B., 2022. Effect of tricyclic 1, 2-thiazine derivatives in neuroinflammation induced by preincubation with lipopolysaccharide or coculturing with microglia-like cells. *Pharmacological Reports*, 74(5), pp.890-908. <https://doi.org/10.1007/s43440-022-00414-8>
- [11] Jasim, S.S., Abdulwahid, J.H., Beebany, S. and Mohammed, B.L., 2023. Synthesis, identification, and antibacterial effect assessment of some new 1, 4-thiazepines, derived from substituted diphenyl acrylamides and diphenyl dienones. *Chemical Methodologies*, 7, pp.509-523. <https://doi.org/10.22034/chemm.2023.392659.1668>
- [12] Dalaf, A.H., Jumaa, F.H., Aftana, M.M., Salih, H.K. and Abd, I.Q., 2022. Synthesis, Characterization, Biological Evaluation, and Assessment Laser Efficacy for New Derivatives of Tetrazole. In *Key Engineering Materials* (Vol. 911, pp. 33-39). Trans Tech Publications Ltd. <https://doi.org/10.4028/p-6849u0>
- [13] Dabholkar, V.V. and Parab, S.D., 2011. Synthesis of chalcones, 1, 3-thiazines and 1, 3-pyrimidines derivatives and their biological evaluation for anti-inflammatory, analgesic and ulcerogenic activity. *The Pharm. Res*, 5, pp.127-143.
- [14] Abdul Wahed Abdul, S.T., Mohammed Jwher, S. and Jamil Nadhem, S., 2024. Preparation, Characterisation and Study of the Molecular Docking of Some Derivatives of the Tetrazole Ring and Evaluation of their Biological Activity. *World of Medicine: Journal of Biomedical Sciences*, 1(7), pp.15-23. Available at <http://eprints.umsida.ac.id/id/eprint/15687>
- [15] Saleh, M.J., Saleh, J.N. and Al-Badrany, K., 2024. Preparation, characterization, and evaluation of the biological activity of pyrazoline derivatives prepared using a solid base catalyst. *European Journal of Modern Medicine and Practice*, 4(7), pp.25-32.

- [16] Saleh, J.N. and Khalid, A., 2023. Synthesis, characterization and biological activity evaluation of some new pyrimidine derivatives by solid base catalyst AL<sub>2</sub>O<sub>3</sub>-OBa. Central Asian Journal of Medical and Natural Science, 4(4), pp.231-239.
- [17] Al-Hadidi, O.A.F., Al-Badrany, K.A. and Al-Bajari, S.A., 2022. Synthesis some of thiazepine compounds from 2-carboxyaldehyde-5-methyl thiophene and study their biological activity on infected male rats epileptic. Journal of Education and Scientific Studies, 2(20).
- [18] Najim, D.M., Al-badrany, K.A. and Saleh, M.K., 2022. Synthesis of some new oxazepine compounds derived from cyanoethyl acetate and study their inhibitory activity against some pathogenic bacterial species. International journal of health sciences, 6(S1), pp.14527-14541. <https://doi.org/10.53730/ijhs.v6nS1.8901>
- [19] Al-Tufah, M.M., Jasim, S.S. and Al-Badrany, K.A., 2020. Synthesis and Antibacterial Evaluation of some New Pyrazole Derivatives. Prof.(Dr) RK Sharma, 20(3), p.178.
- [20] Kumar, S., Arora, A., Sapra, S., Kumar, R., Singh, B.K. and Singh, S.K., 2024. Recent advances in the synthesis and utility of thiazoline and its derivatives. RSC advances, 14(2), pp.902-953. <https://doi.org/10.1039/D3RA06444A>
- [21] Talluh, A.W.A.S., Saleh, J.N. and Saleh, M.J., 2024. Preparation, Characterization and Evaluation of Biological Ac-tivity and Study of Molecular Docking of Some New Thiazoli-dine Derivatives. World of Science: Journal on Modern Research Technologies, 3(2), pp.49-57. Available at <https://univerpubl.com/index.php/woscience>
- [22] Saleh, M.J. and Al-Badrany, K.A., 2023. Preparation, characterization of new 2-oxo pyran derivatives by AL<sub>2</sub>O<sub>3</sub>-OK solid base catalyst and biological activity evaluation. Central Asian Journal of Medical and Natural Science, 4(4), pp.222-230.
- [23] Abdul Wahed Abdul, S.T., Mohammed, J.S., Jamil Nadhem, S. and Khalid, A.B., 2024. Preparation, characterization, and evaluation of the biological activity of new 2, 3-dihydroquinazoline-4-one derivatives. European Journal of Modern Medicine and Practice, 4(4), pp.326-332. Available at <http://eprints.umsida.ac.id/id/eprint/15678>
- [24] Talluh, A. W. A. S. (2024). Preparation, Characterization, Evaluation of Biological Activity, and Study of Molecular Docking of Azetidine Derivatives. Central Asian Journal of Medical and Natural Science, 5(1), 608-616.
- [25] Al-Suhail, R.G.A. and Ali, L.F., 2021. Statistical analysis of COVID-19 pandemic across the provinces of Iraq. Iraqi Journal of Science, pp.811-824.